Electronic Supplementary Material (ESI) for Nanoscale.

Supporting Information

Hot Electron Injection into Semiconducting Polymers in Polymer Based-Perovskite Solar Cells and their Fate

Jesús Jiménez-López,†[a,b] Bianka M. D. Puscher,†[c] Werther Cambarau,[a] Rainer H. Fink,[c] Emilio Palomares,*[a,d] and Dirk M. Guldi*[c]

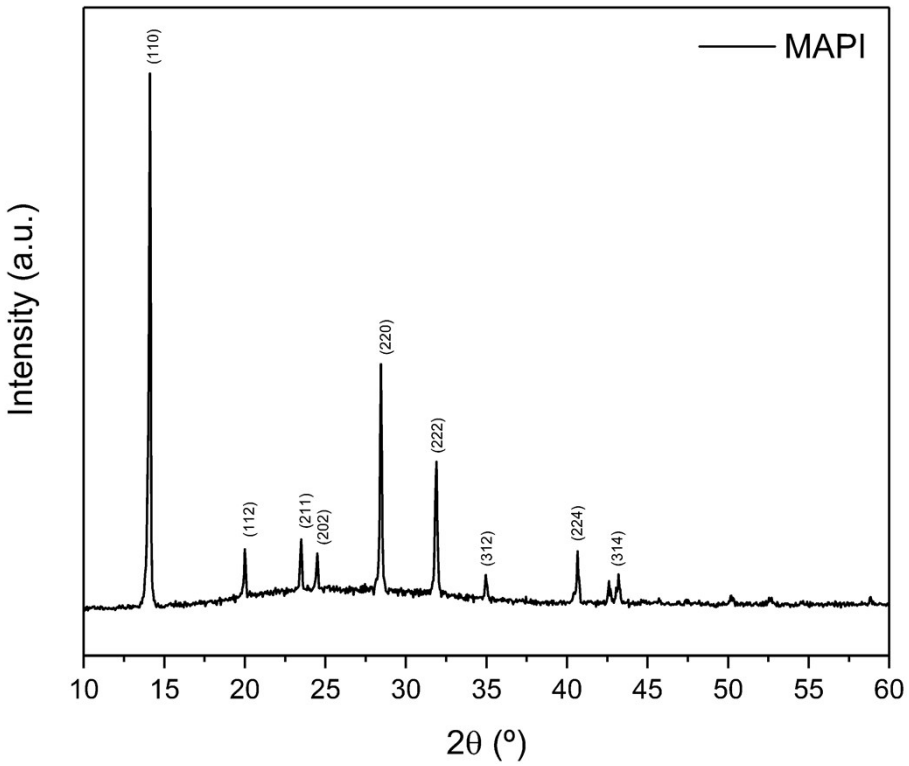

Figure S1. XRD pattern of MAPI measured on a glass film (bump between 15-35º). Peak assignment has been done according to Guo et al.[1]

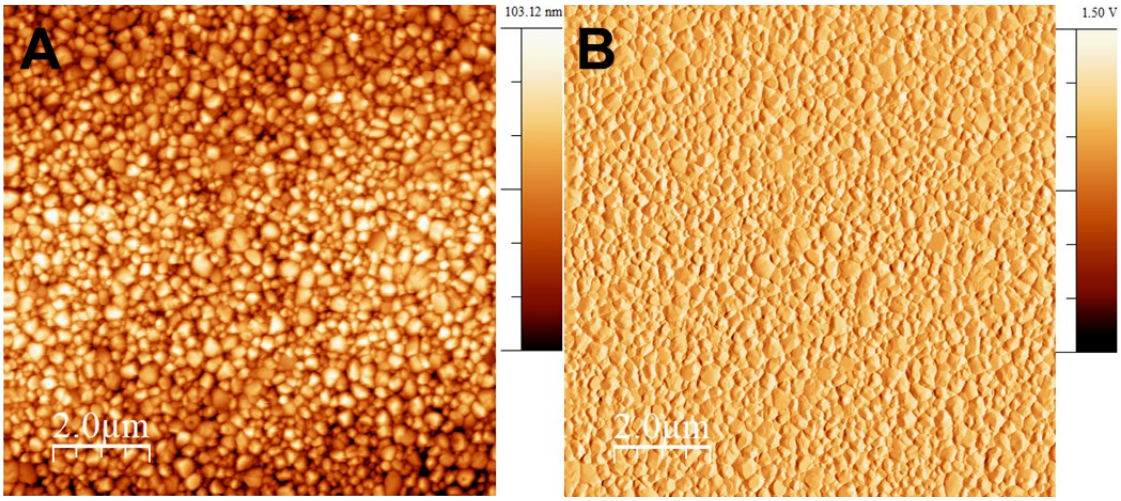

Figure S2. AFM images of MAPI films with topography image (A) and voltage amplitude (B).

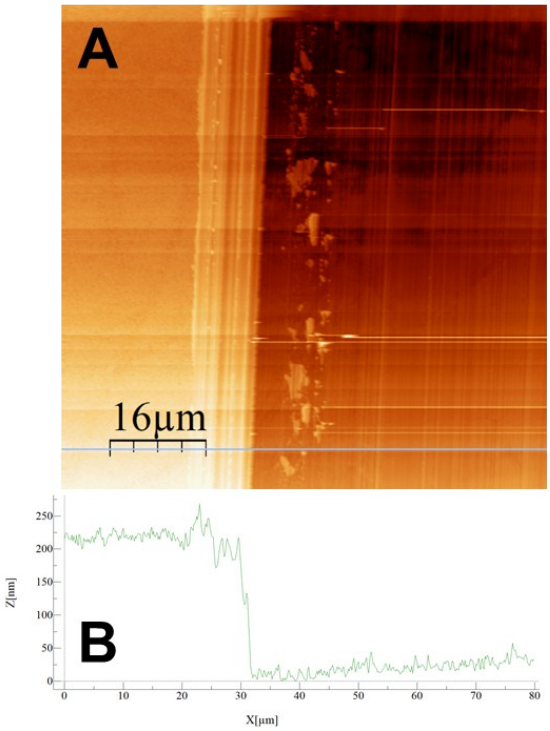

Figure S3. AFM image of MAPI film (A) used to calculate the thickness of the sample (B).

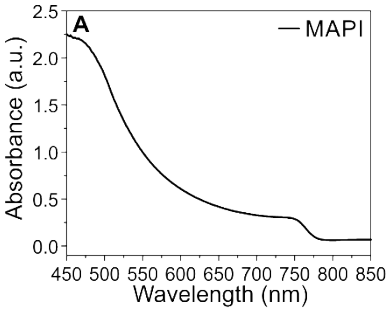

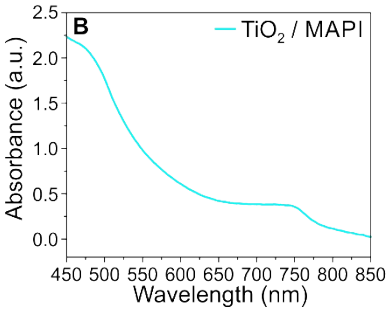

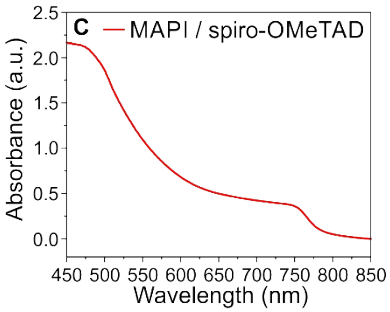

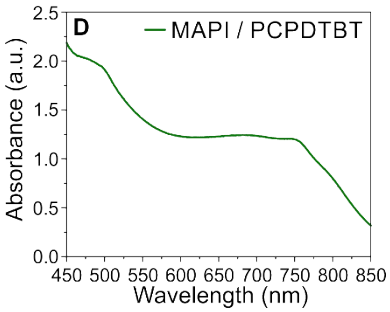

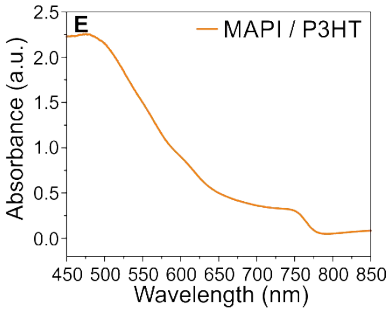

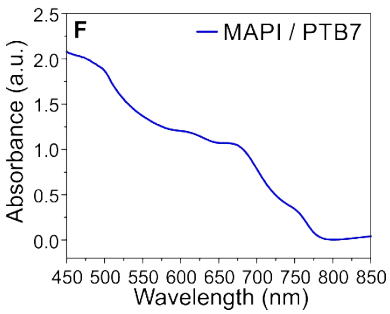

Figure S4. UV-vis absorption spectra of the different films used in this study. (A) MAPI, (B) TiO_2/MAPI, (C) MAPI/spiro-OMeTAD, (D) MAPI/PCPDTBT, (E) MAPI/P3HT, and (F) MAPI/PTB7.

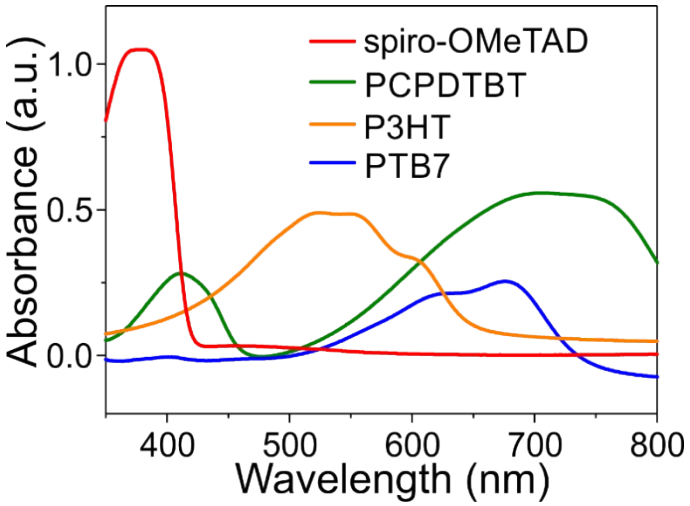

Figure S5. UV-Vis spectra of spiro-OMeTAD, PCPDTBT, P3HT, and PTB7.

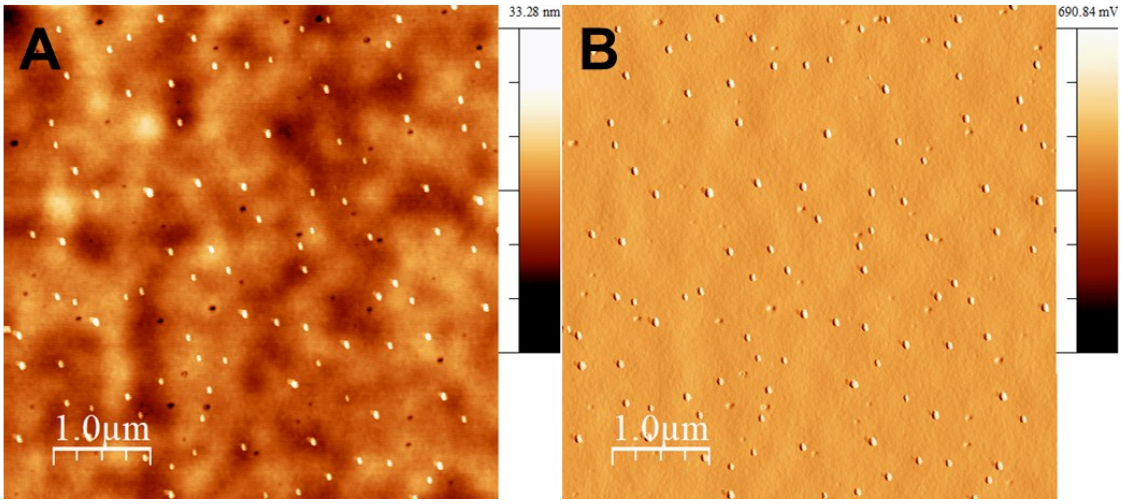

Figure S6. AFM images of MAPI/spiro-OMeTAD films on the spiro-OMeTAD surface with topography image (A) and voltage amplitude (B).

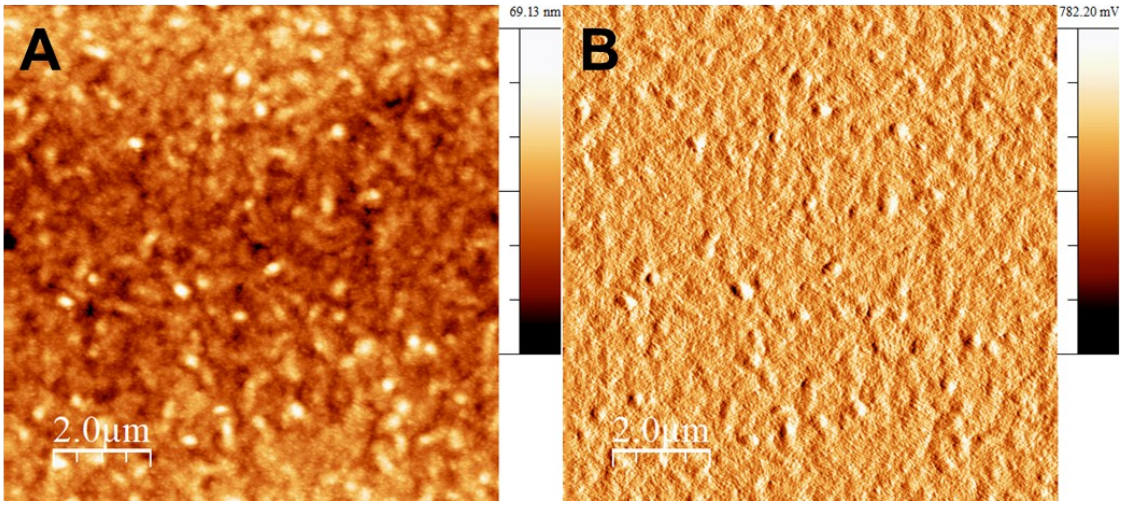

Figure S7. AFM images of MAPI/PCPDTBT films on the PCPDTBT surface with topography image (A) and voltage amplitude (B).

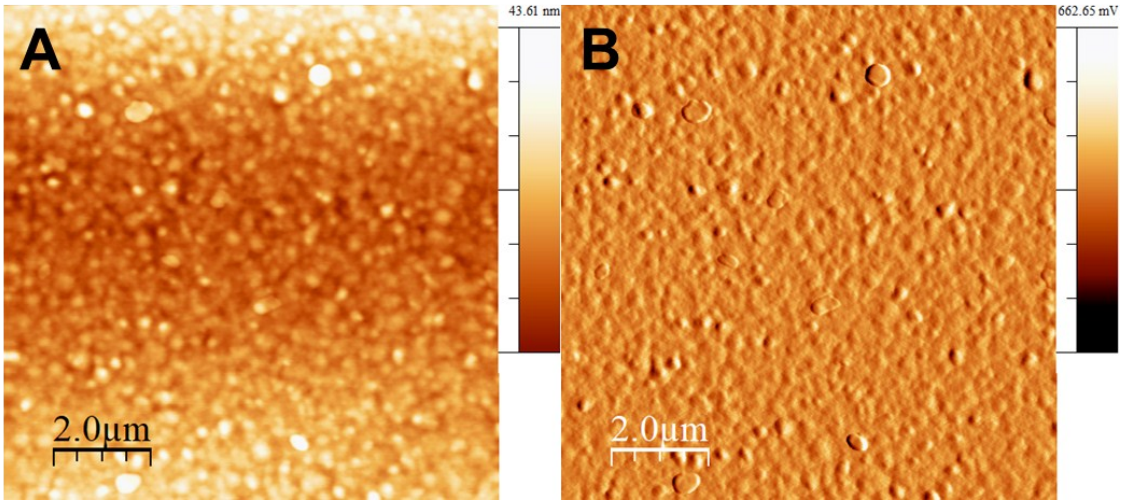

Figure S8. AFM images of MAPI/P3HT films on the P3HT surface with topography image (A) and voltage amplitude (B).

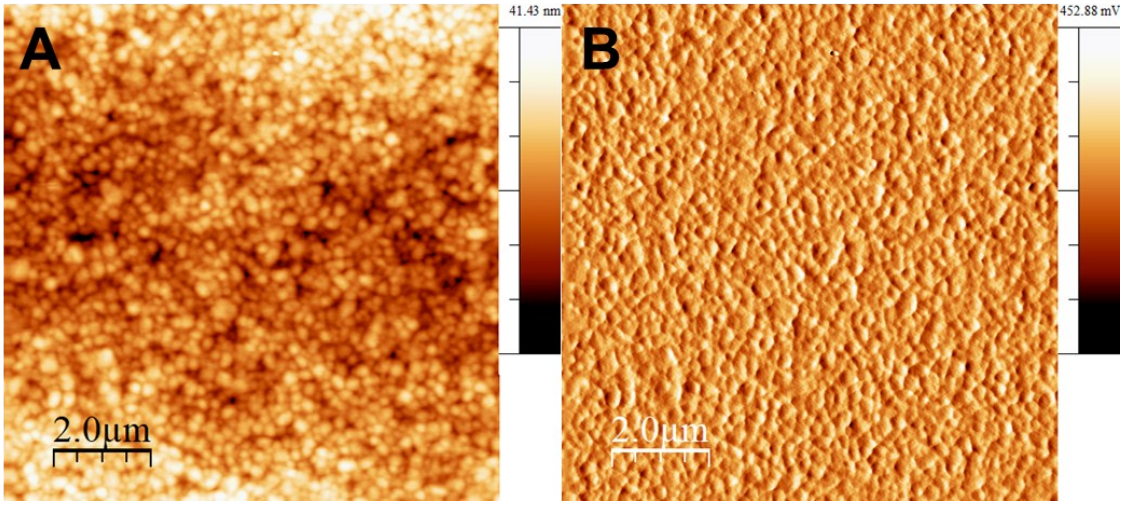

Figure S9. AFM images of MAPI/PTB7 films on the PTB7 surface with topography image (A) and voltage amplitude (B).

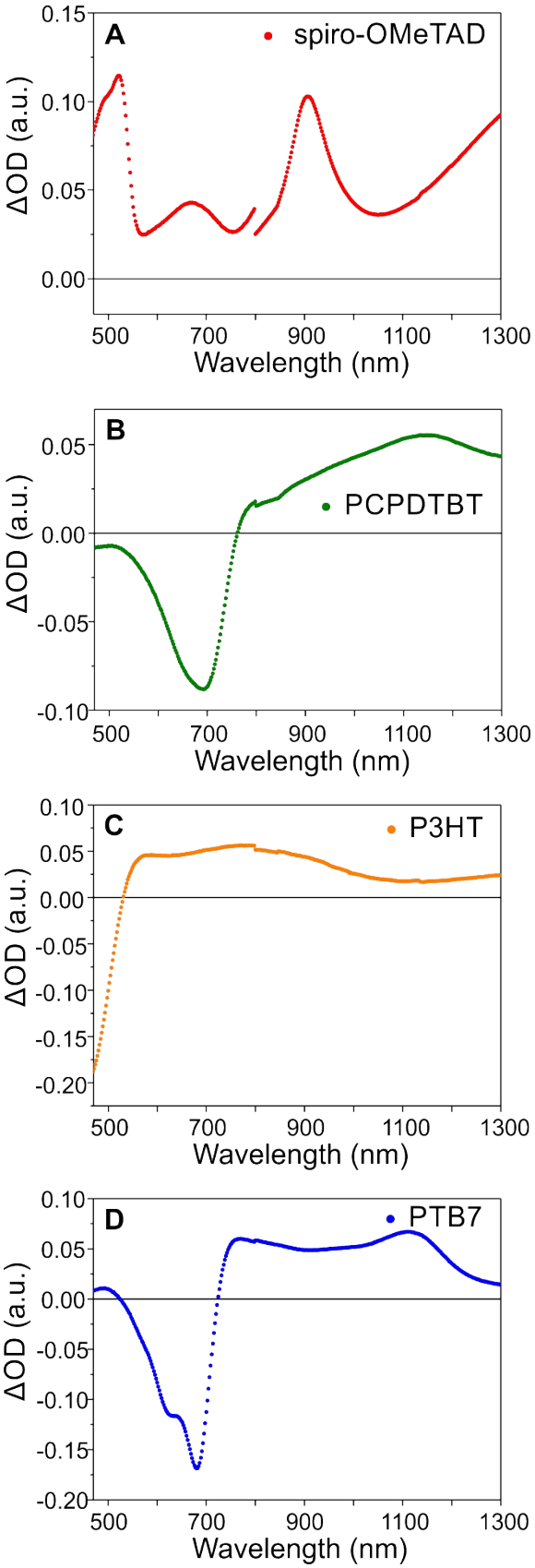

Figure S10. Differential absorption spectra obtained by spectroelectrochemical oxidation revealing the features for the different HTM, (A) spiro-OMeTAD, (B) PCPDTBT, (C) P3HT, and (D) PTB7, measured in solution. Different voltages were applied for each HTM in order to obtain the desired spectra of their oxidized forms ($V_{spiro\text{-}OMeTAD}$ = +0.27 V; $V_{PCPDTBT}$ = +0.07 V; V_{P3HT} = +1.07 V; V_{PTB7} = +1.52 V, all potentials *vs.* Fc/Fc^{+}).

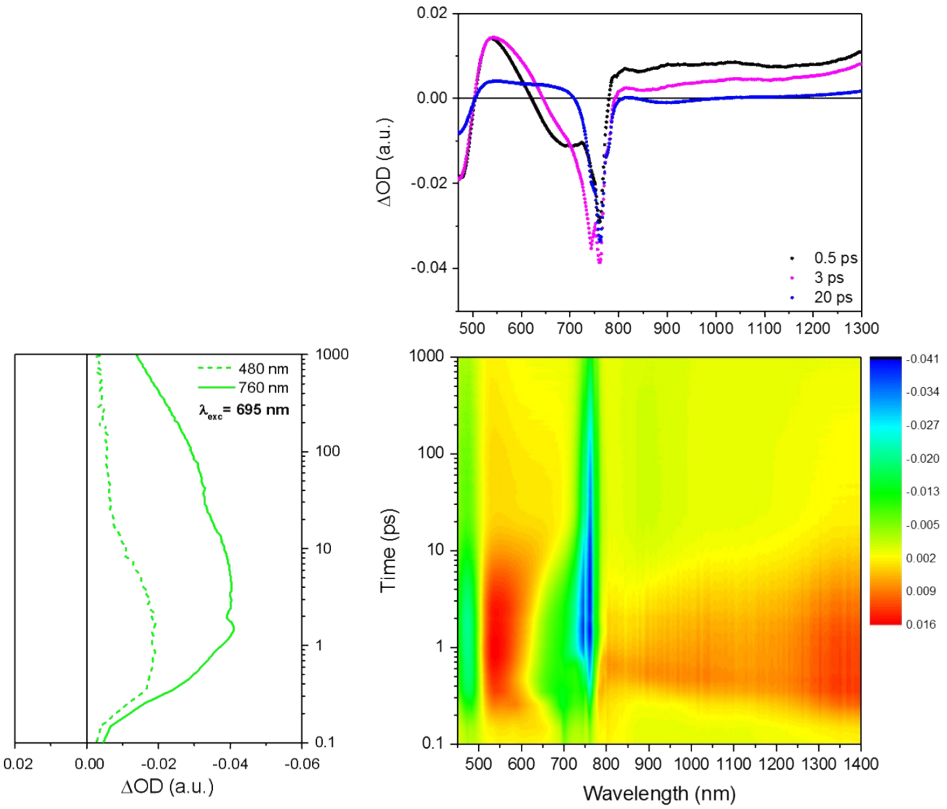

Figure S11. Fs-TA spectra of MAPI films with λ_{exc} = 695 nm. Differential absorption spectra (top) shown in the lower right with time delays of 0.5 ps (black), 3 ps (violet), and 20 ps (blue). Time absorption profiles (lower left) of the spectra shown in the lower right at 480 nm (dashed green) and 760 nm (solid green).

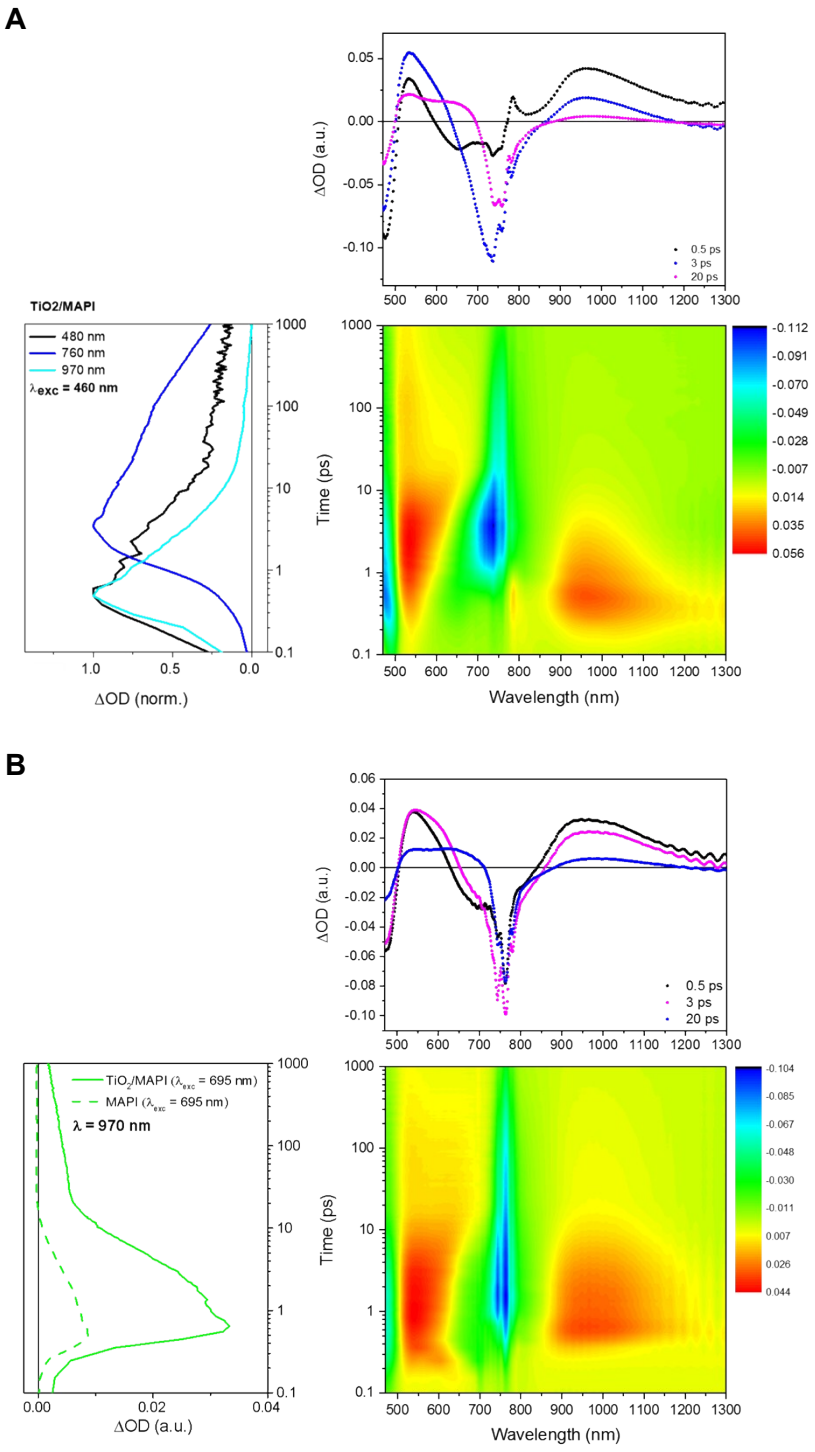

Figure S12. Fs-TA spectra of TiO_2/MAPI films with λ_{exc} = 460 (A) and 695 nm (B). Differential absorption spectra (top) shown in the lower right with time delays of 0.5 (black), 3 (violet) and 20 ps (blue). Time absorption profiles (lower left) of the hot electron PIA signal at 480 nm (black in (A)), 760 nm (blue in (B)), and 970 nm (cyan in (A)) for TiO_2/MAPI as well as at 970 nm for TiO_2/MAPI (solid green in (B)) and MAPI (dashed green in (B)), showing the electron injection into the TiO_2 layer.

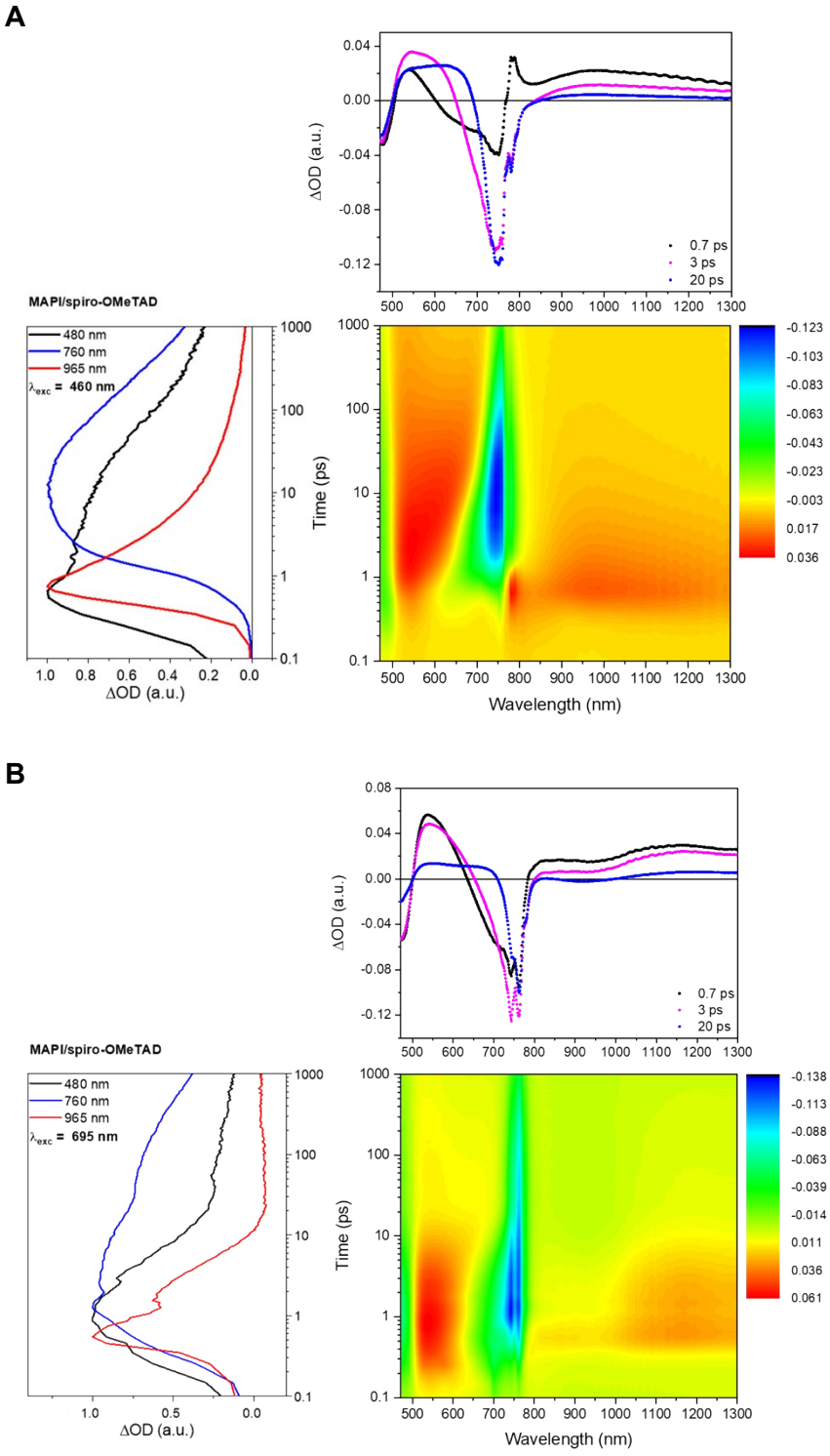

Figure S13. Fs-TA spectra of MAPI/spiro-OMeTAD films with λ_{exc} = 460 (A) and 695 nm (B). Differential absorption spectra (top) shown in the lower right with time delays of 0.7 (black), 3 (purple), and 20 ps (blue). Time absorption profiles (lower left) of the spectra shown in the lower right at 480 nm (black), 760 nm (blue), and 965 nm (red).

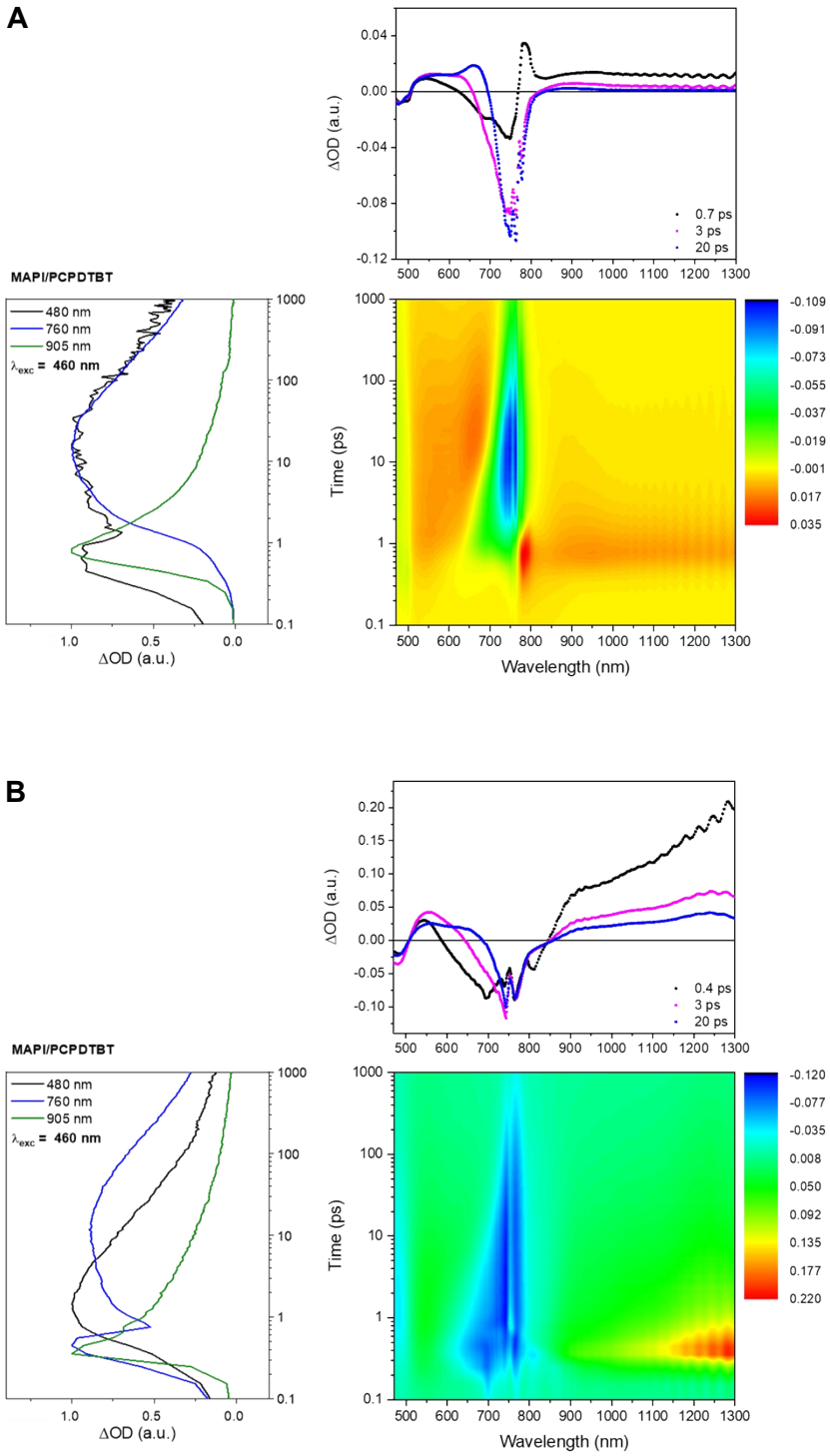

Figure S14. Fs-TA spectra of MAPI/PCPDTBT films with λ_{exc} = 460 (A) and 695 nm (B). Differential absorption spectra (top) shown in the lower right with time delays of 0.7 (black), 3 (purple), and 20 ps (blue) in (a) and 0.4 (black), 3 (purple), and 20 ps (blue). Time absorption profiles (lower left) of the spectra shown in the lower right at 480 nm (black), 760 nm (blue), and 905 nm (green).

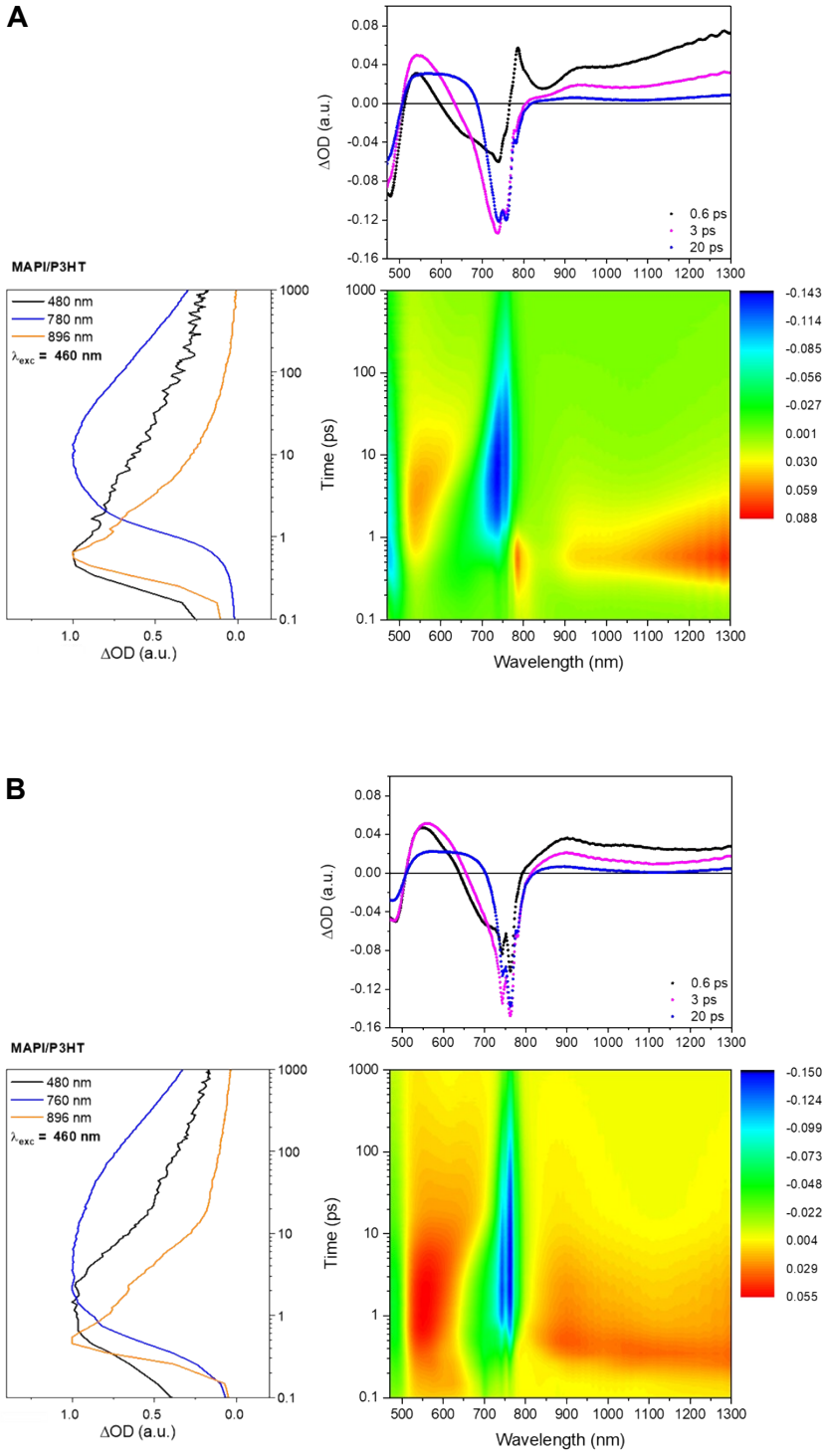

Figure S15. Fs-TA spectra of MAPI/P3HT films with λ_{exc} = 460 (A) and 695 nm (B). Differential absorption spectra (top) shown in the lower right with time delays of 0.6 (black), 3 (purple), and 20 ps (blue). Time absorption profiles (lower left) of the spectra shown in the lower right at 480 nm (black), 760 nm (blue), and 896 nm (orange).

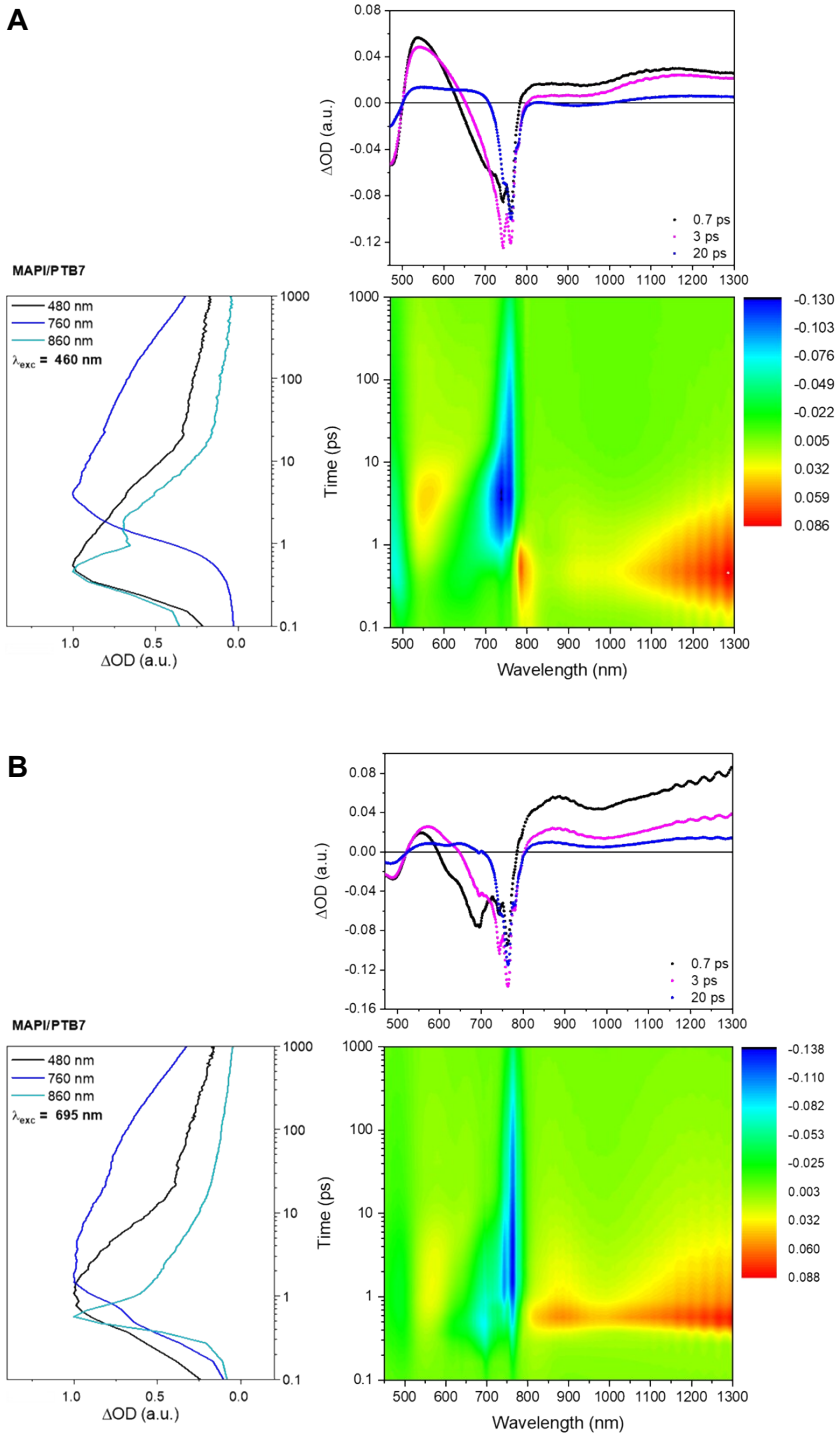

Figure S16. Fs-TA spectra of MAPI/PTB7 films with λ_{exc} = 460 (A) and 695 nm (B). Differential absorption spectra (top) shown in the lower right with time delays of 0.7 (black), 3 (purple), and 20 ps (blue). Time absorption profiles (lower left) of the spectra shown in the lower right at 480 nm (black), 760 nm (blue), and 860 nm (cyan).

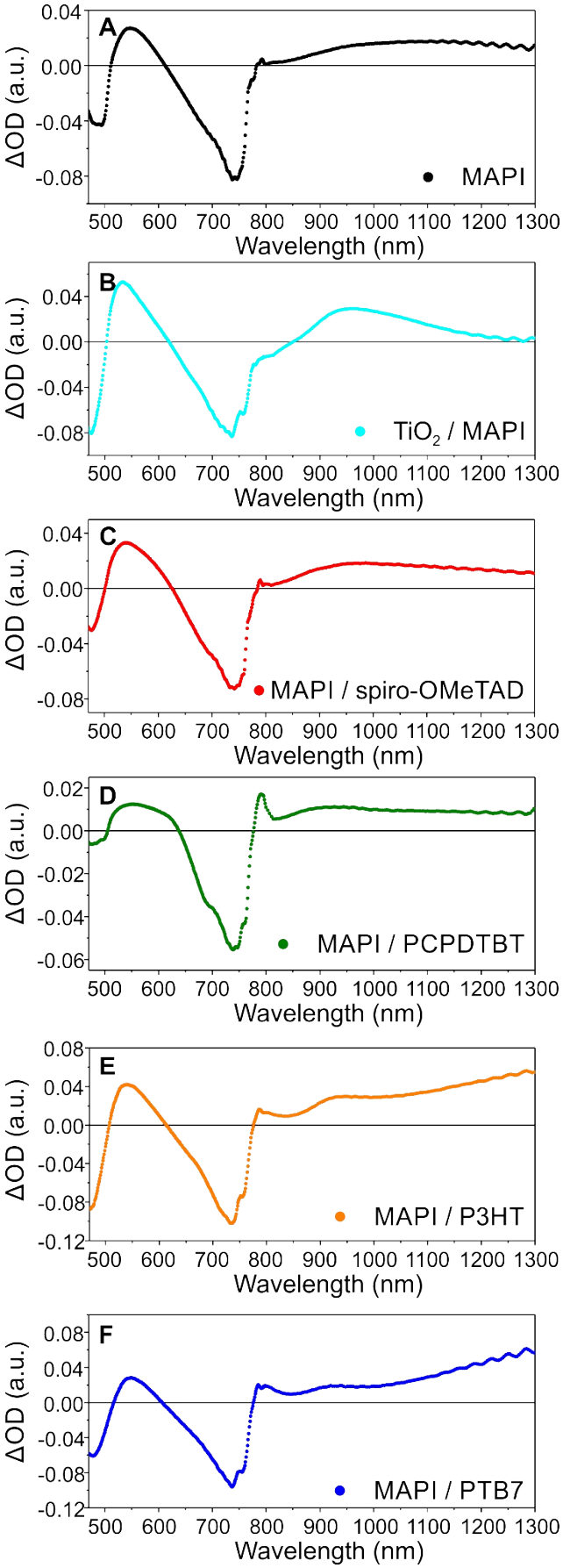

Figure S17. Comparison of the differential absorption spectra in both vis- and NIR-region of different films (MAPI (A), TiO_2/MAPI (B), MAPI/spiro-OMeTAD (C), MAPI/PCPDTBT (D), MAPI/P3HT (E), and MAPI PTB7 (F)) at 1.2 ps by means of pumping at λ_{exc} = 460 nm and a laser fluence of 130 μJ cm^{-2}.

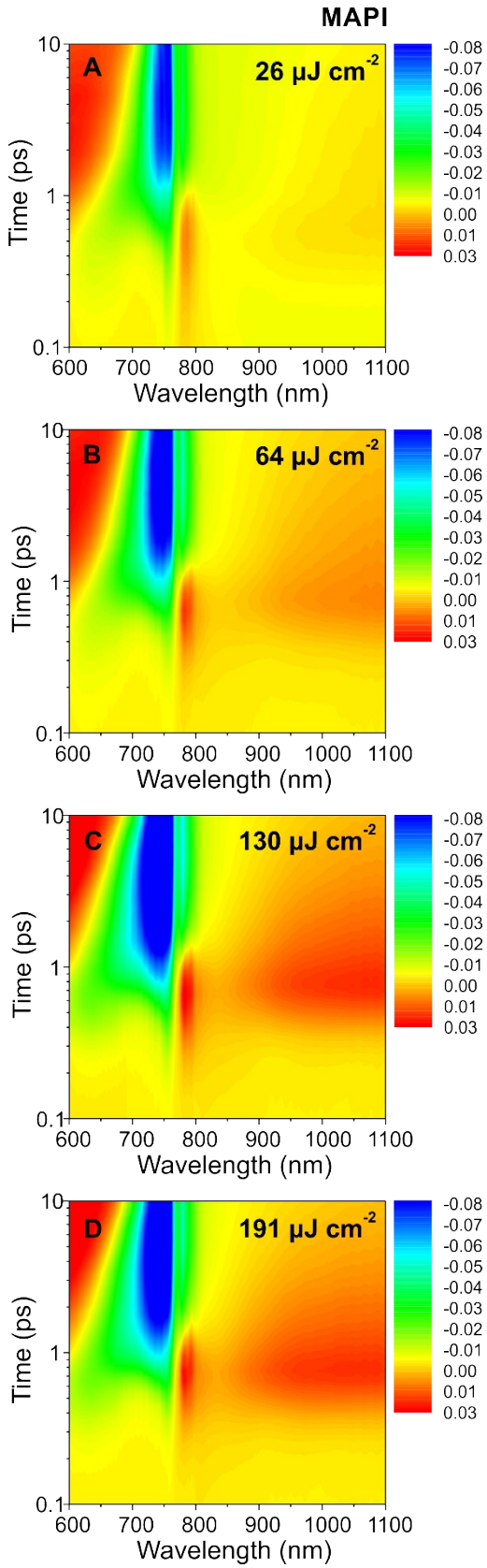

Figure S18. Fs-TA spectra of a MAPI film with λ_{exc} = 460 and increasing laser fluence from 26 (A), 64 (B), 130 (C), and 191 μJ cm^{-2} (D).

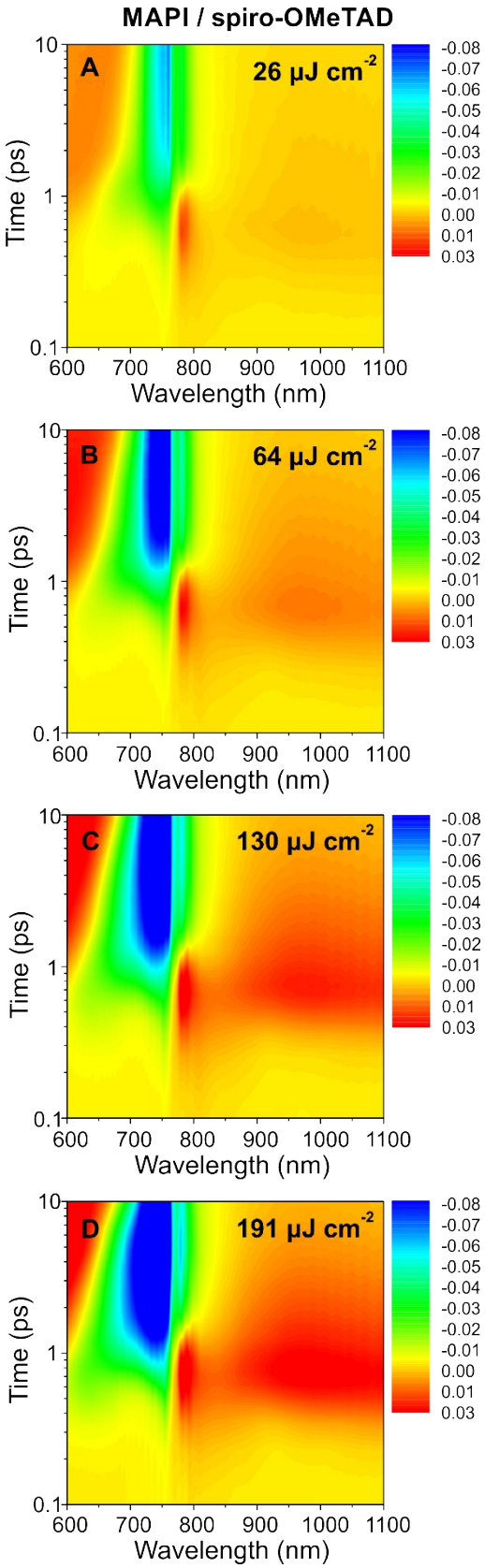

Figure S19. Fs-TA spectra of a MAPI/spiro-OMeTAD film with λ_{exc} = 460 and increasing laser fluence from 26 (A), 64 (B), 130 (C), and 191 µJ cm^{-2} (D).

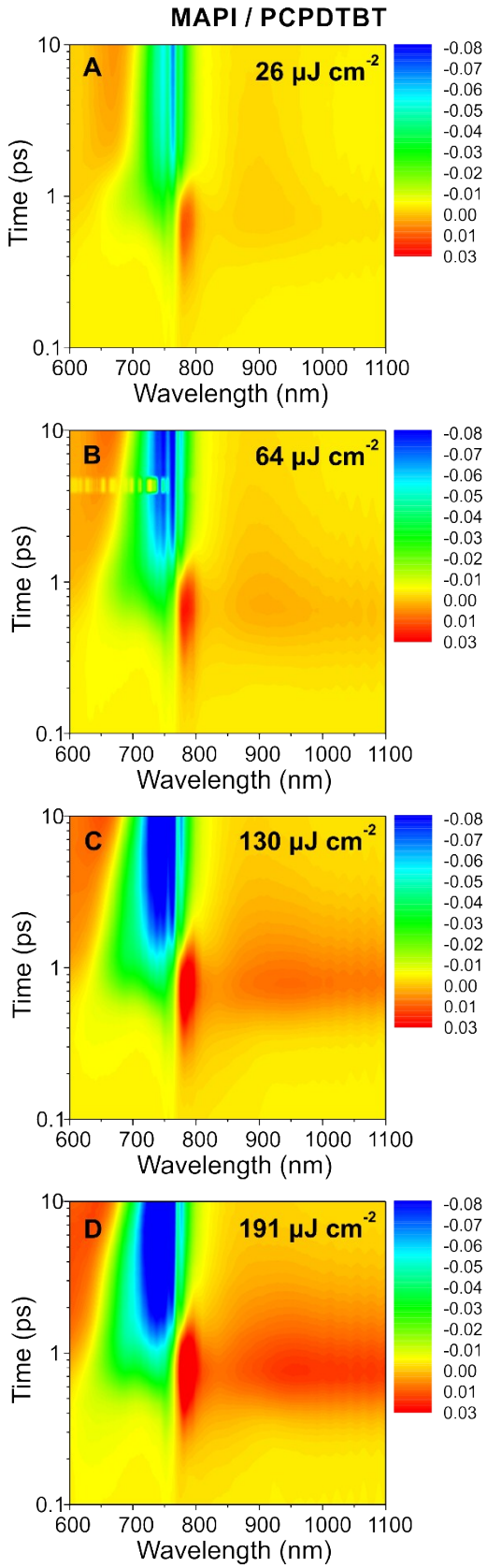

Figure S20. Fs-TA spectra of a MAPI/PCPDTBT film with λ_{exc} = 460 and increasing laser fluence from 26 (A), 64 (B), 130 (C), and 130 µJ cm^{-2} (D).

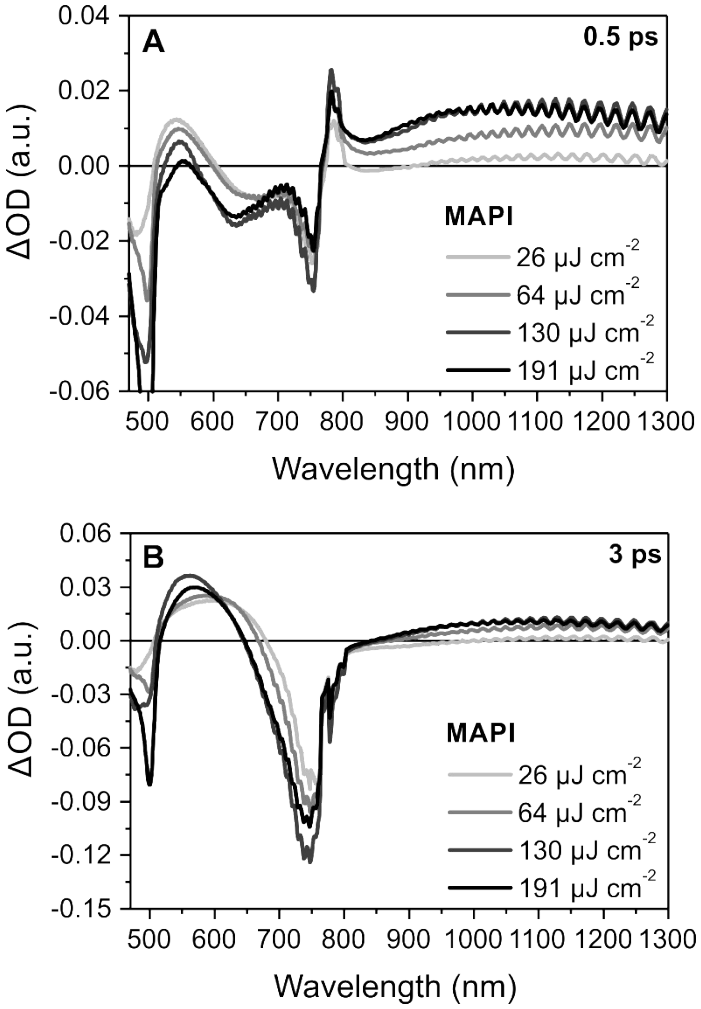

Figure S21. Comparison of differential spectra at 0.5 (A) and 3 ps (B) with λ_{exc} = 460 nm and increasing laser fluences from 26 to 191 μJ cm^{-2} of MAPI.

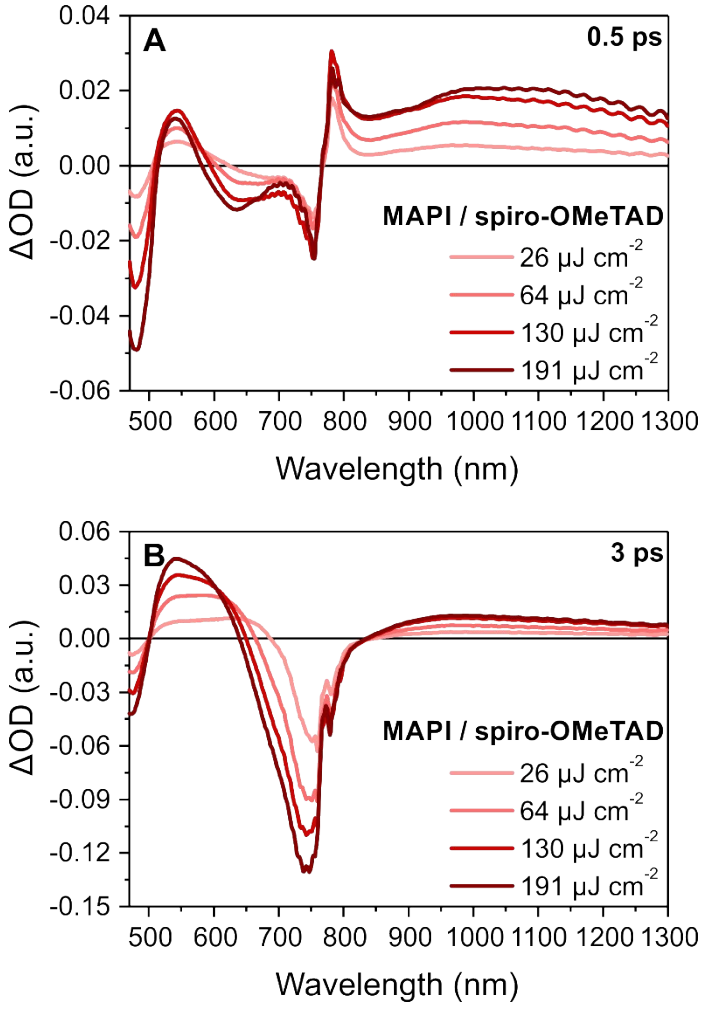

Figure S22. Comparison of differential spectra at 0.5 (A) and 3 ps (B) with λ_{exc} = 460 nm and increasing laser fluences from 26 to 191 μJ cm^{-2} of MAPI/spiro-OMeTAD.

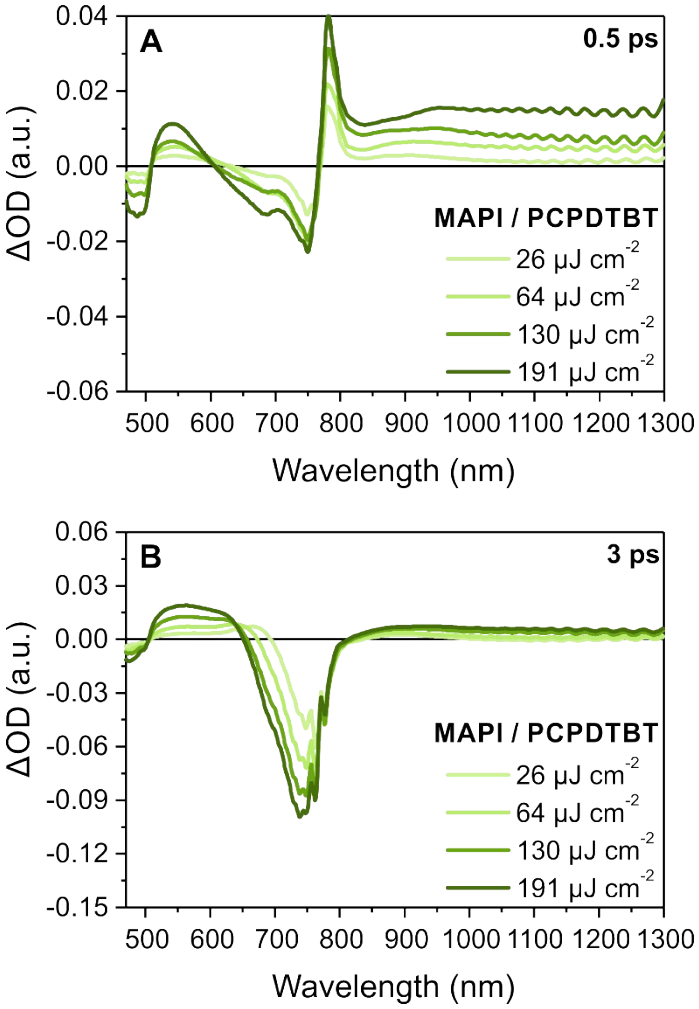

Figure S23. Comparison of differential spectra at 0.5 (A) and 3 ps (B) with λ_{exc} = 460 nm and increasing laser fluences from 26 to 191 μJ cm^{-2} of MAPI/PCPDTBT.

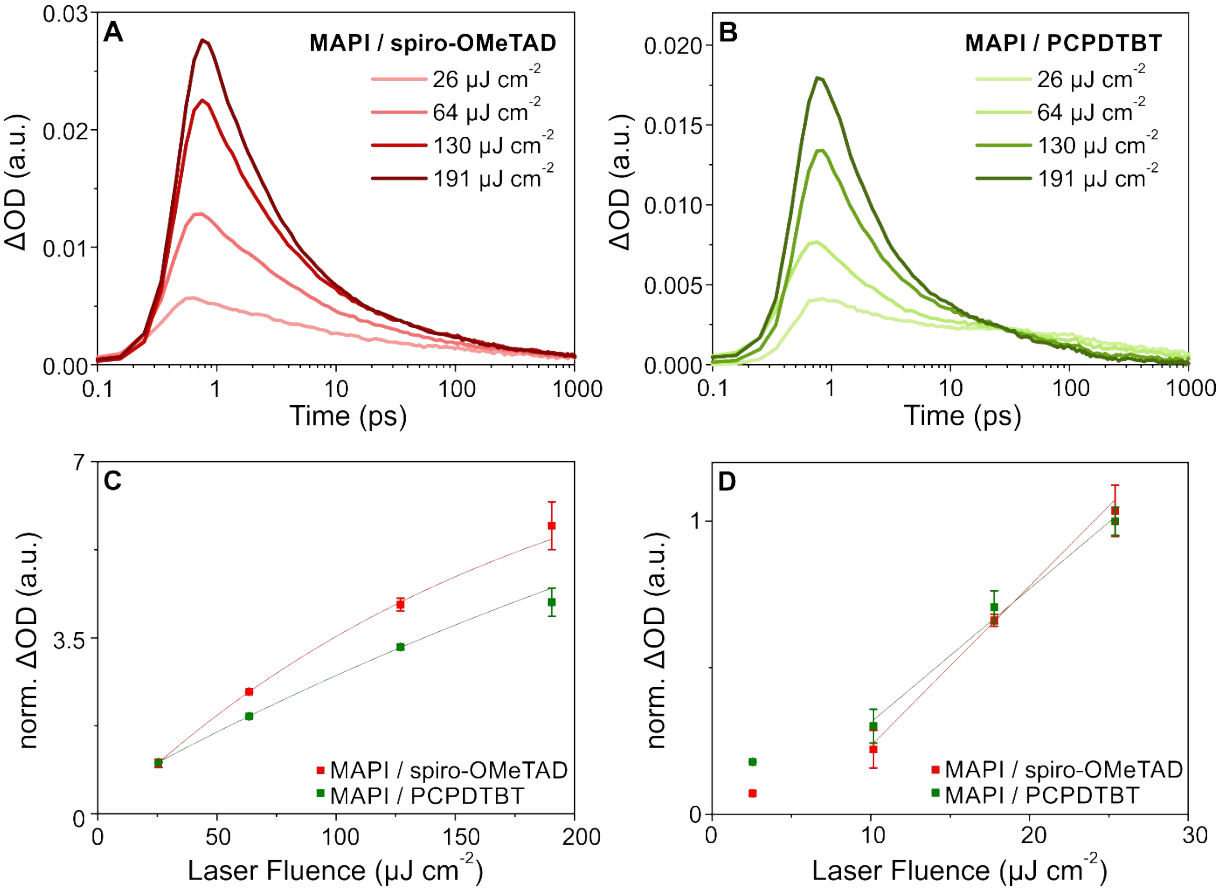

Figure S24. Time absorption profiles of spiro-OMeTAD's (A) and PCPDTBT's (B) polaron signals at 965 and 905 nm, respectively, with increasing laser fluences from 26 to 191 µJ cm^{-2}. The exponential and linear increase of the PIA at its maximum (MAPI/spiro-OMeTAD, red, and MAPI/PCPDTBT, green) is given in dependence of the laser fluence above (C) and below (D) 26 µJ cm^{-2}. The data was normalized according to 26 µJ cm^{-2}.

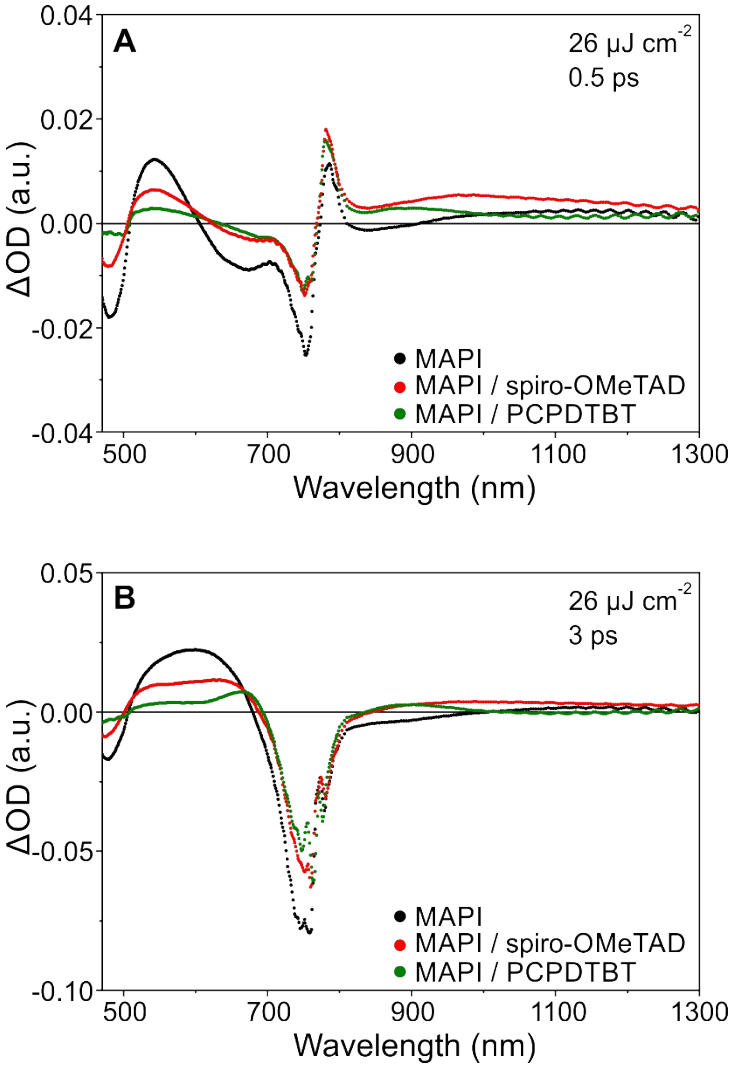

Figure S25. Comparison of differential spectra at 0.5 (A) and 3 ps (B) by means of pumping at λ_{exc} = 460 nm with a laser fluences of 26 μJ cm^{-2} of MAPI (black), MAPI/spiro-OMeTAD (red), and MAPI/PCPDTBT (green).

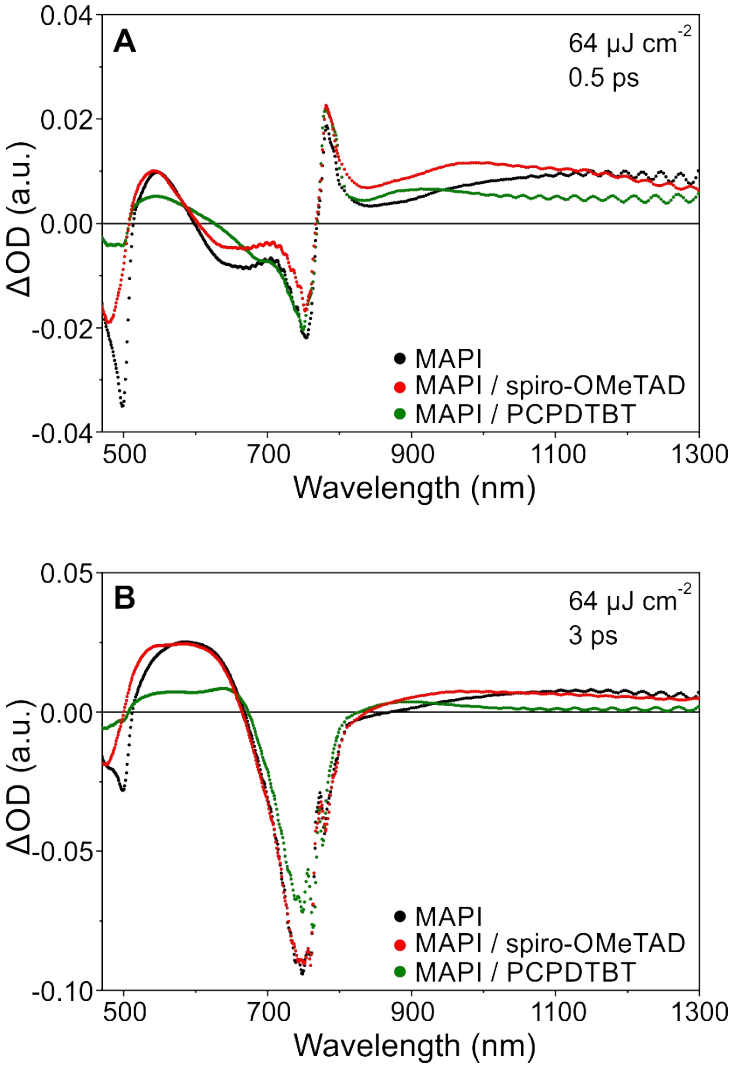

Figure S26. Comparison of differential spectra at 0.5 (A) and 3 ps (B) by means of pumping at λ_{exc} = 460 nm with a laser fluences of 64 μJ cm^{-2} of MAPI (black), MAPI/spiro-OMeTAD (red), and MAPI/PCPDTBT (green).

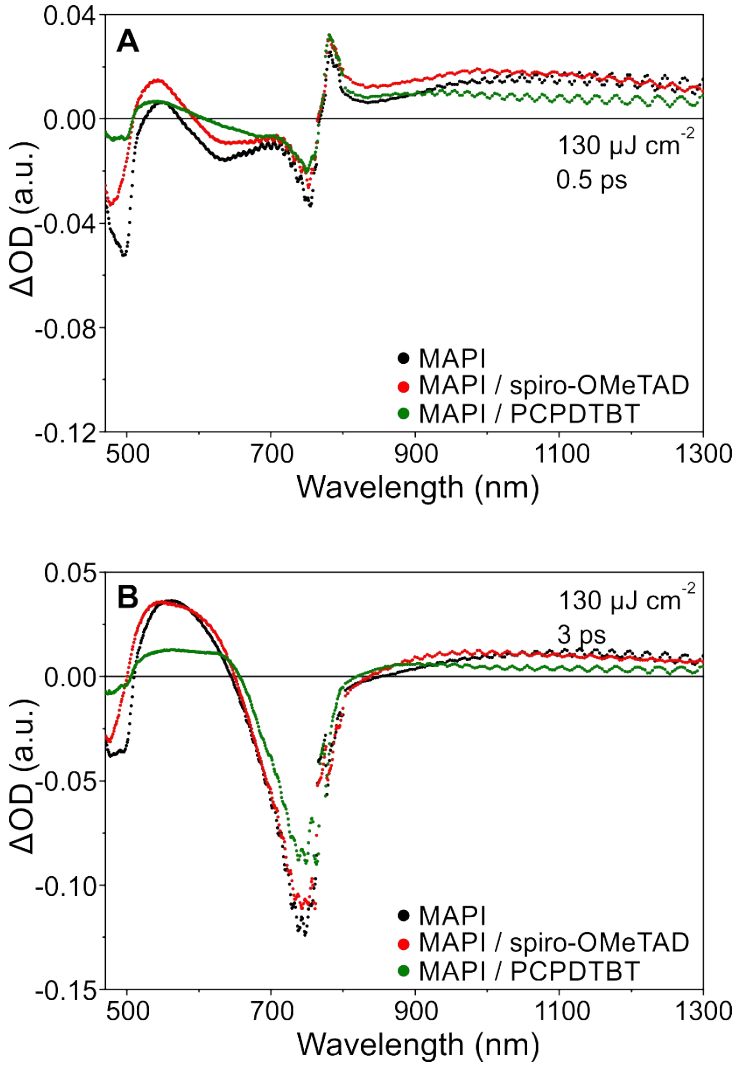

Figure S27. Comparison of differential spectra at 0.5 (A) and 3 ps (B) by means of pumping at λ_{exc} = 460 nm with a laser fluences of 130 µJ cm^{-2} of MAPI (black), MAPI/spiro-OMeTAD (red), and MAPI/PCPDTBT (green).

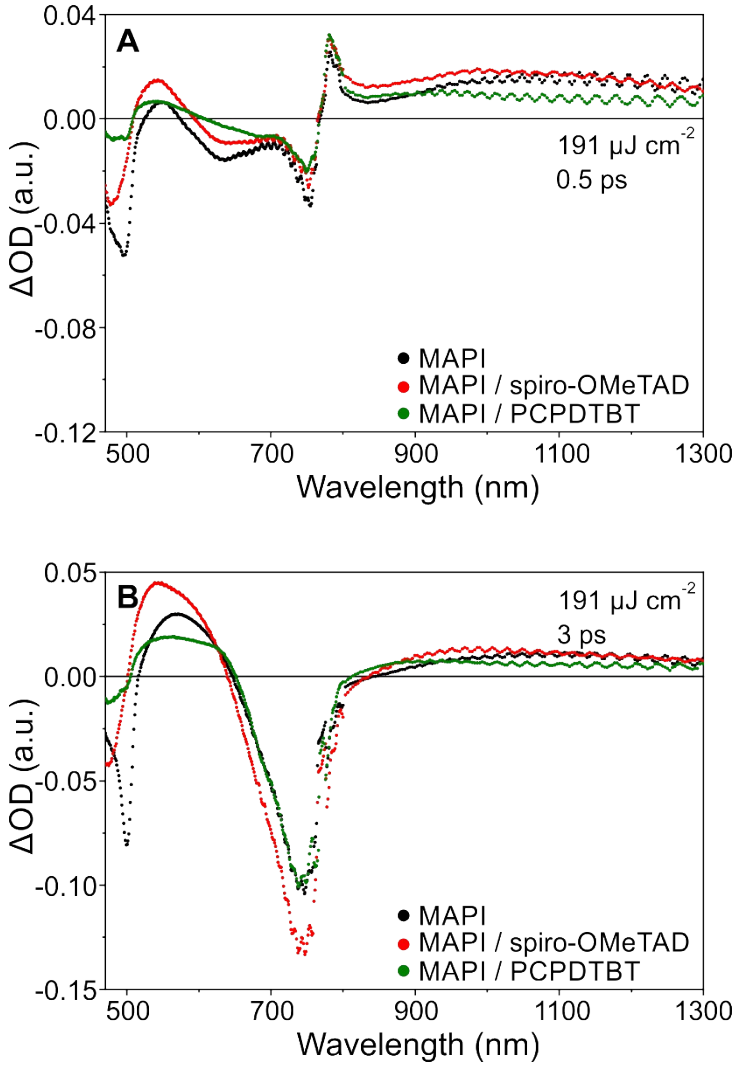

Figure S28. Comparison of differential spectra at 0.5 (A) and 3 ps (B) by means of pumping at λ_{exc} = 460 nm with a laser fluences of 191 µJ cm^{-2} of MAPI (black), MAPI/spiro-OMeTAD (red), and MAPI/PCPDTBT (green).

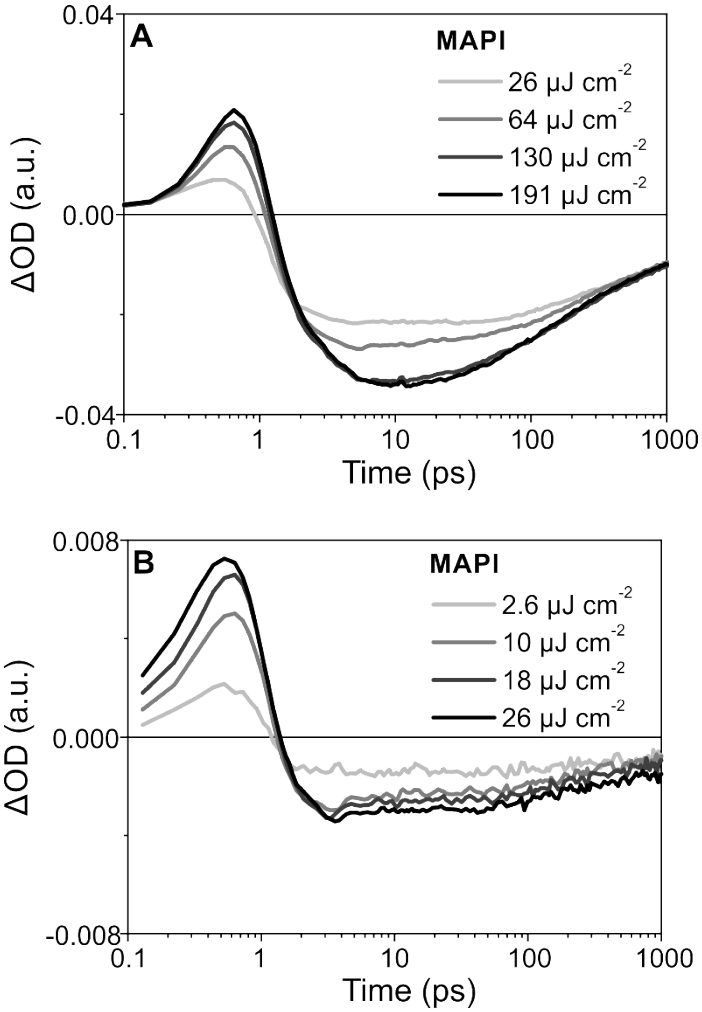

Figure S29. Kinetic traces at 785 nm of MAPI with λ_{exc} = 460 nm and increasing the laser fluence from 26 to 191 μJ cm^{-2} (A, MAPI film thickness of 200 nm) and 2.6 to 26 μJ cm^{-2} (B, MAPI film thickness of 100 nm).

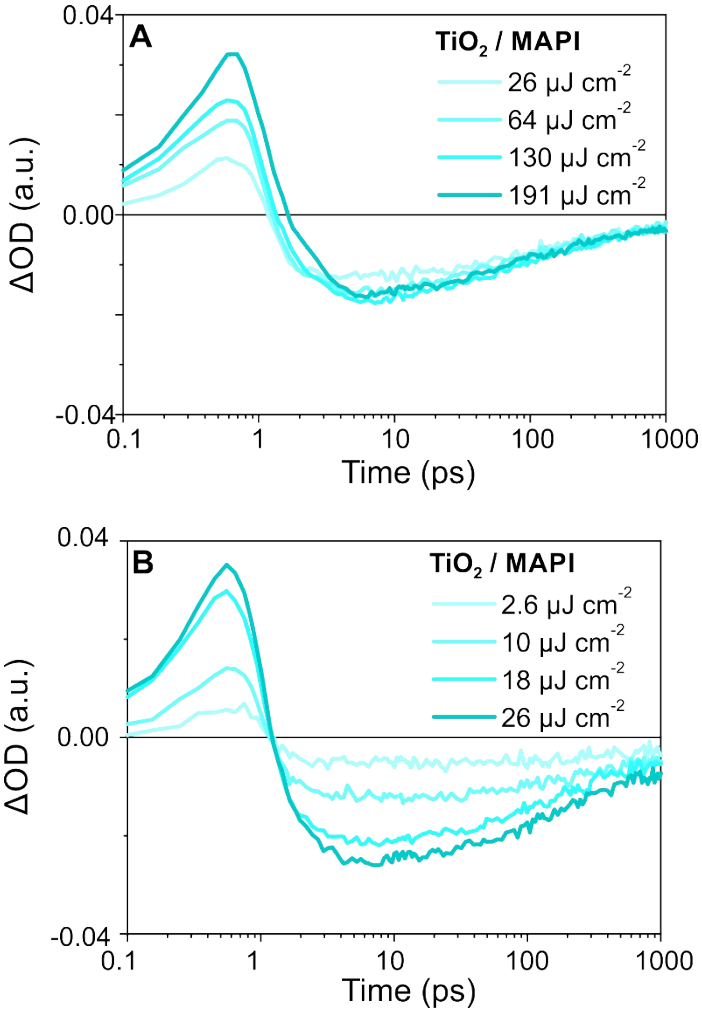

Figure S30. Kinetic traces at 785 nm of TiO_2/MAPI with λ_{exc} = 460 nm and increasing the laser fluence from 26 to 191 μJ cm^{-2} (A, MAPI film thickness of 200 nm) and 2.6 to 26 μJ cm^{-2} (B, MAPI film thickness of 100 nm).

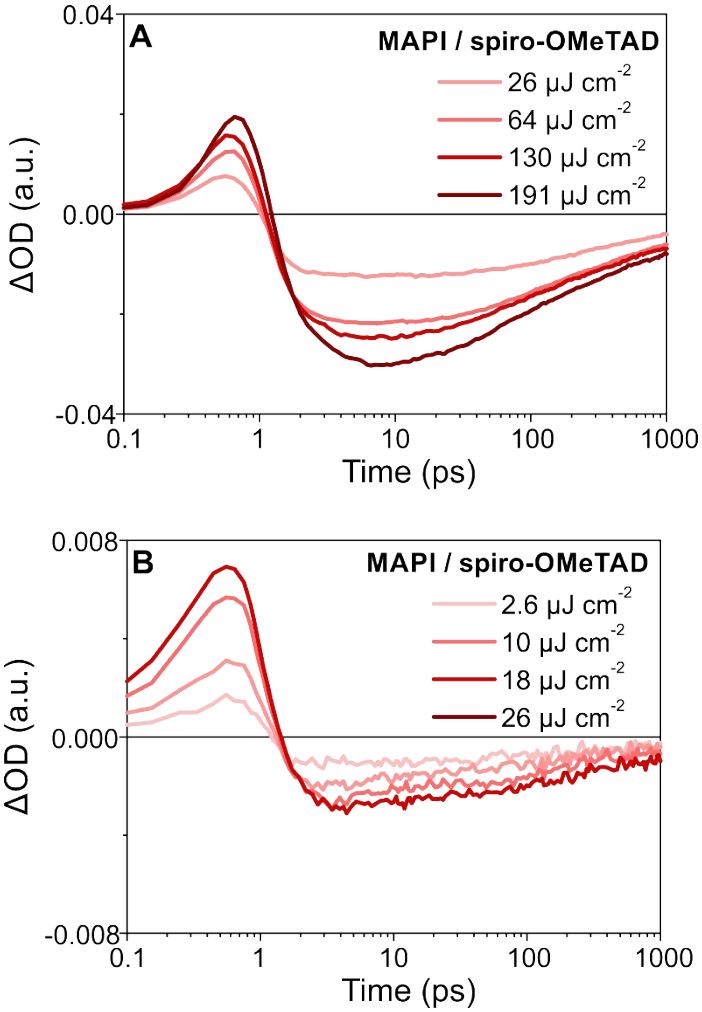

Figure S31. Kinetic traces at 785 nm of MAPI/spiro-OMeTAD with λ_{exc} = 460 nm and increasing the laser fluence from 26 to 191 μJ cm^{-2} (A, MAPI film thickness of 200 nm) and 2.6 to 26 μJ cm^{-2} (B, MAPI film thickness of 100 nm).

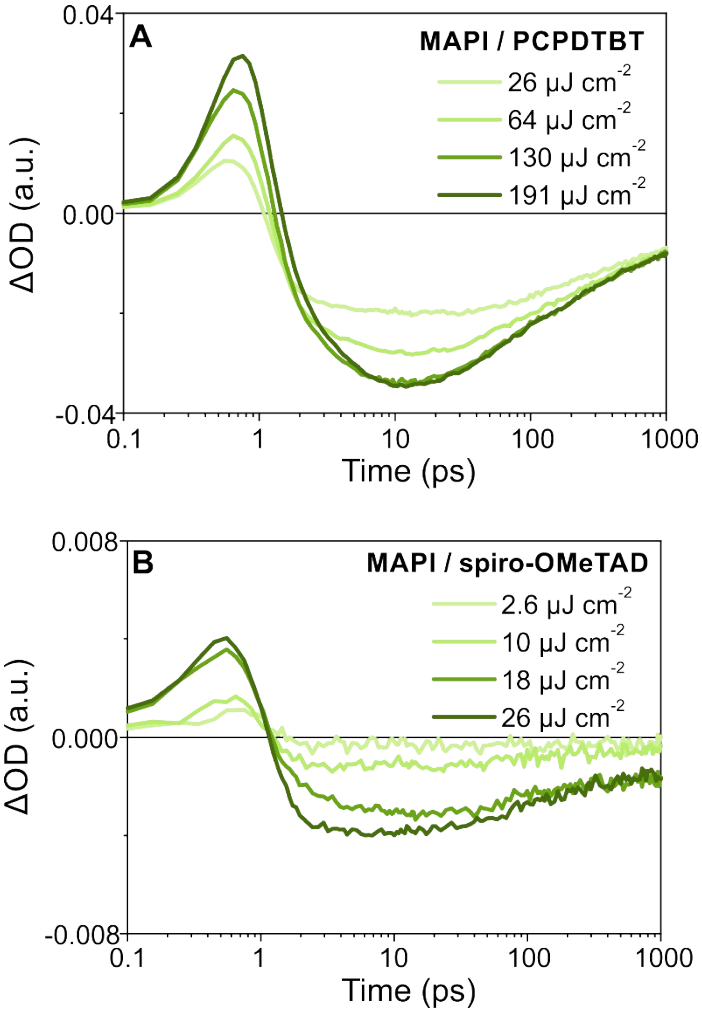

Figure S32. Kinetic traces at 785 nm of MAPI/PCPDTBT with λ_{exc} = 460 nm and increasing the laser fluence from 26 to 191 μJ cm^{-2} (A, MAPI film thickness of 200 nm) and 2.6 to 26 μJ cm^{-2} (B, MAPI film thickness of 100 nm).

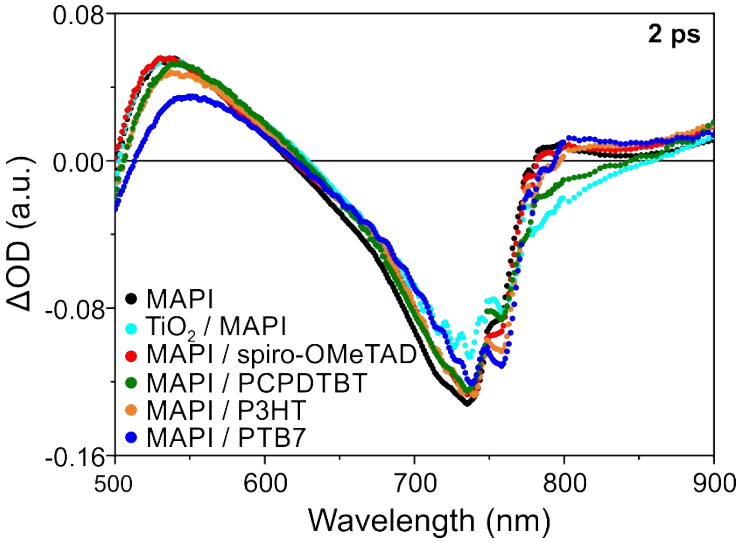

Figure S33. Comparison of differential spectra at 2 ps obtained for MAPI, TiO_2/MAPI, MAPI/spiro-OMeTAD, MAPI/PCPDTBT, MAPI/P3HT, and MAPI/PTB7 by means of pumping at λ_{exc} = 460 nm with a laser fluence of 130 μJ cm^{-2}.

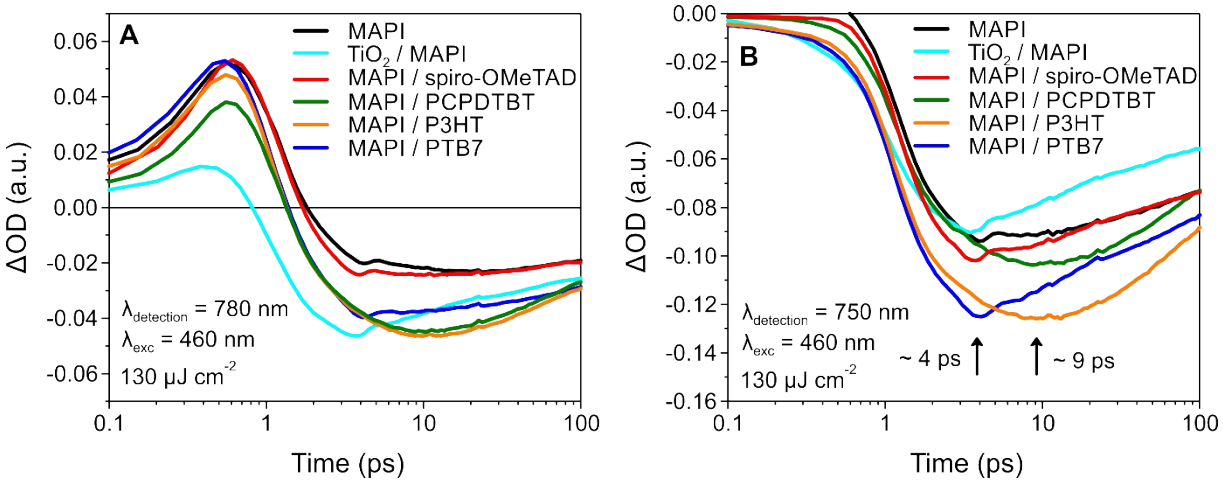

Figure S34. Kinetic traces (0.1 to 100 ps) obtained for MAPI, TiO_2/MAPI, MAPI/spiro-OMeTAD, MAPI/PCPDTBT, MAPI/P3HT, and MAPI/PTB7 by means of pumping at λ_{exc} = 460 nm with a laser fluence of 130 μJ cm^{-2} and probing at the 780 nm PIA (A) and the 760 nm GSB (B).

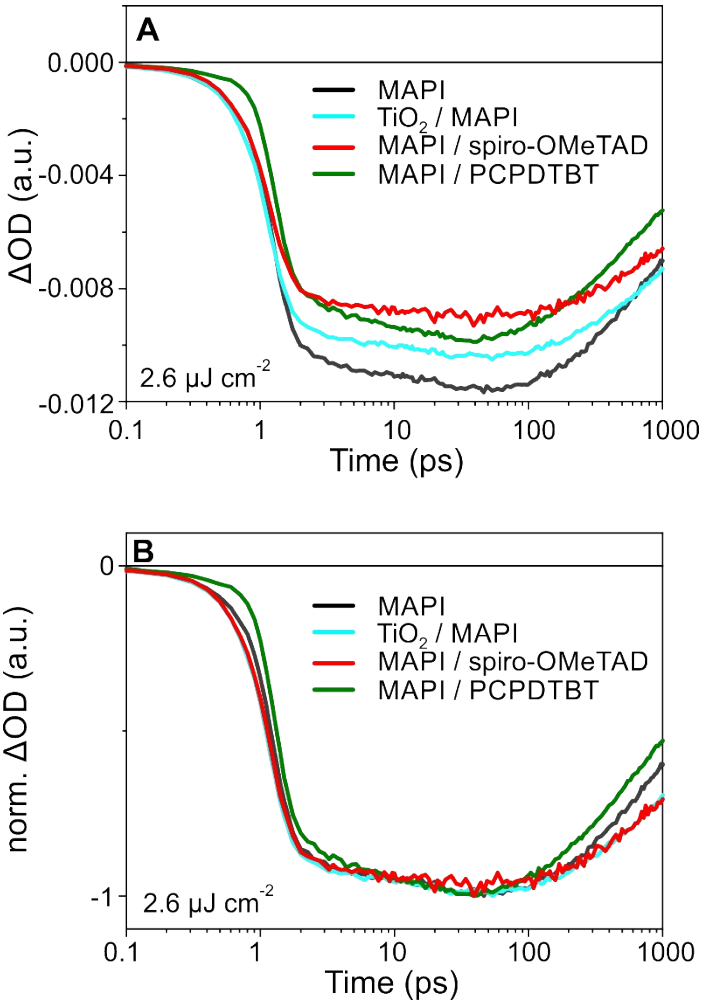

Figure S35. Kinetic traces (A) and normalized kinetic traces (B) (0.1 to 100 ps) obtained for MAPI, TiO_2/MAPI, MAPI/spiro-OMeTAD and MAPI/PCPDTBT by means of pumping at λ_{exc} = 460 nm with a laser fluences of 2.6 μJ cm^{-2} and probing at the 750 nm GSB.

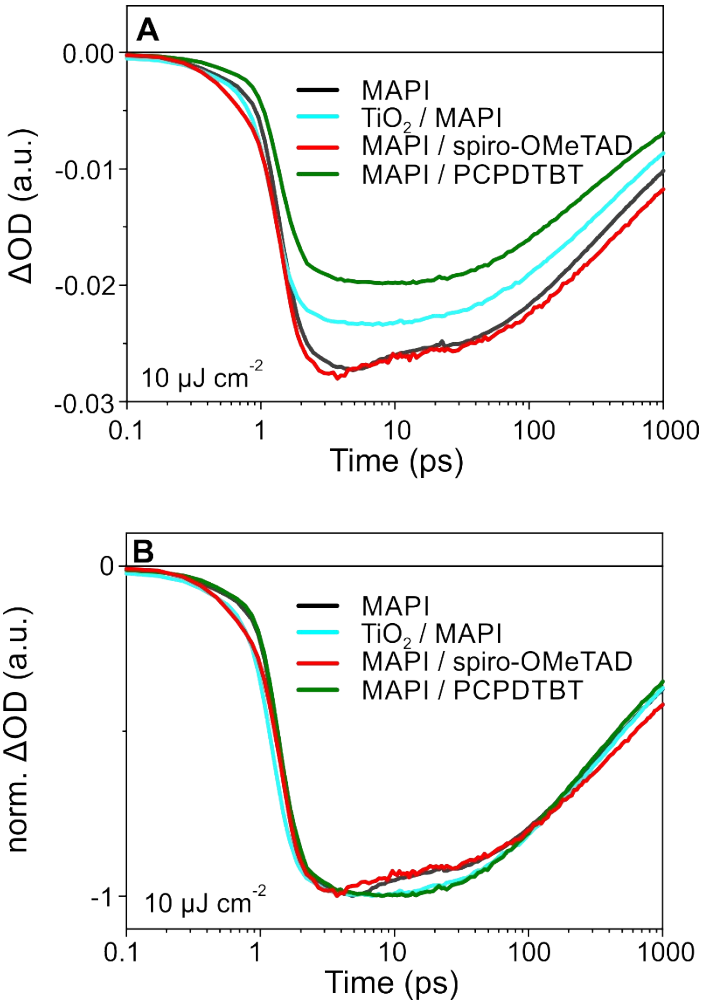

Figure S36. Kinetic traces (A) and normalized kinetic traces (B) (0.1 to 100 ps) obtained for MAPI, TiO_2/MAPI, MAPI/spiro-OMeTAD and MAPI/PCPDTBT by means of pumping at λ_{exc} = 460 nm with a laser fluences of 10 μJ cm^{-2} and probing at the 750 nm GSB.

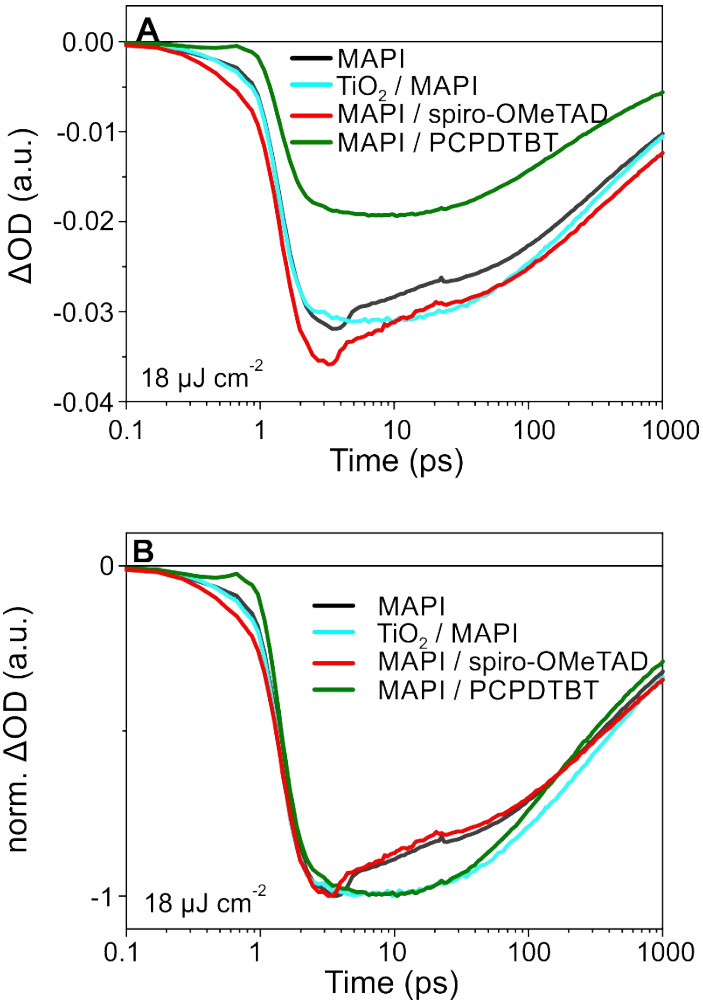

Figure S37. Kinetic traces (A) and normalized kinetic traces (B) (0.1 to 100 ps) obtained for MAPI, TiO_2/MAPI, MAPI/spiro-OMeTAD and MAPI/PCPDTBT by means of pumping at λ_{exc} = 460 nm with a laser fluences of 18 μJ cm^{-2} and probing at the 750 nm GSB.

Table S1. HOMO values of TiO_2 and PCPDTBT, charge (electron) injection rates derived from the fast component in the kinetic traces decay of the reduced species of the ETM. HOMO and LUMO values taken from our work[2].

ETM	HOMO[2] values (eV)	LUMO[2] values (eV)	Charge injection rate 10^{11} (s^{-1})
TiO_2	-7.4	-4.2	10.0 ± 0.3
PCPDTBT	-5.3	-3.55	7.1 ± 0.2

Data Analysis

The kinetics were derived from a tri-exponential fit according to equation 1. An example is given, showing the time absorption profiles at 965 nm (black) and its fit (red) of MAPI:spiro-OMeTAD.

$$y = A_1*\exp(-x/t_1) + A_2*\exp(-x/t_2) + A_3*\exp(-x/t_3) + y_0 \quad (1)$$

$$k = 1/t \quad (2)$$

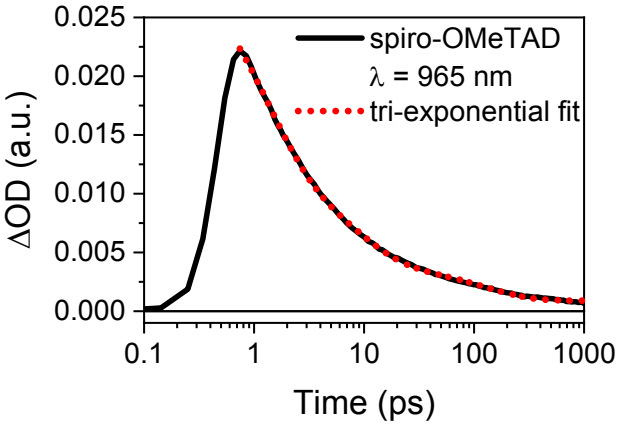

Parameter	
y_0	$8.95*10^{-4} \pm 0.23*10^{-4}$
A_1	$0.019 \pm 2.37*10^{-4}$
t_1	1.123 ± 0.031
A_2	$0.009 \pm 2.01*10^{-4}$
t_2	8.059 ± 0.279
A_3	$0.003 \pm 0.71*10^{-4}$
t_3	$122.26 \pm 4.9*10^{-4}$
Reduced Chi²	$1.12*10^{-8}$
Adj. R^2	0.9996

References

1 X. Guo, C. McCleese, C. Kolodziej, A. C. S. Samia, Y. Zhao and C. Burda, *Dalt. Trans.*, 2016, **45**, 3806–3813.

2 J. Jiménez-López, W. Cambarau, L. Cabau and E. Palomares, *Sci. Rep.*, 2017, **7**, 6101.